Ligand-Mediated Biofilm Formation via Enhanced Physical Interaction Between a Diguanylate Cyclase and Its Receptor

David Giacalone[1], T. Jarrod Smith[1], Alan J. Collins[1], Holger Sondermann[3], Lori J. Koziol[2], and George A. O'Toole[1,*]

[1]Department of Microbiology and Immunology, Geisel School of Medicine at Dartmouth, Hanover, NH 03755

[2]Department of Biology, New England College, Henniker, NH 03242

[3]Department of Molecular Medicine, College of Veterinary Medicine, Cornell University, Ithaca, NY 14853

*Corresponding author: George A. O'Toole; address: Geisel School of Medicine at Dartmouth, Dept. of Microbiology and Immunology, Remson 202, 66 North College St., Hanover, NH 03755; phone: 603-650-1248; email: georgeo@Dartmouth.edu

Key words: biofilm, c-di-GMP, receptor, *Pseudomonas fluorescens*, CACHE domain, signaling

Abstract. The second messenger, cyclic dimeric GMP (c-di-GMP) regulates biofilm formation for many bacteria. The binding of c-di-GMP by the inner-membrane protein LapD controls biofilm formation, and the LapD receptor is central to a complex network of c-di-GMP-mediated biofilm formation. In this study, we examine how c-di-GMP signaling specificity by a diguanylate cyclase (DGC), GcbC, is achieved via interactions with the LapD receptor and by small ligand sensing via GcbC's calcium channel chemotaxis (CACHE) domain. We provide evidence that biofilm formation is stimulated by the environmentally relevant organic acid citrate (and a related compound, isocitrate) in a GcbC-dependent manner through enhanced GcbC-LapD interaction, which results in increased LapA localization to the cell surface. Furthermore, GcbC shows little ability to synthesize c-di-GMP in isolation. However, when LapD is present GcbC activity is significantly enhanced ~8-fold, indicating that engaging the LapD receptor stimulates the activity of this DGC; citrate-enhanced GcbC-LapD interaction further stimulates c-di-GMP synthesis. We propose that the I-site of GcbC serves two roles beyond allosteric control of this enzyme: promoting GcbC-LapD interaction and stabilizing the active conformation of GcbC in the GcbC-LapD complex. Finally, given that LapD can interact with a dozen different DGCs of *P. fluorescens*, many of which have ligand-binding domains, the ligand-mediated enhanced signaling via LapD-GcbC interaction described here is likely a conserved mechanism of signaling in this network. Consistent with this idea, we identify a second example of ligand-mediated enhancement of DGC-LapD interaction that promotes biofilm formation.

Importance. In many bacteria, dozens of enzymes produce the dinucleotide signal c-di-GMP, however it is unclear how undesired crosstalk is mitigated in the context of this soluble signal,

41 and how c-di-GMP signaling is regulated by environmental inputs. We demonstrate that GcbC,
42 a DGC, shows little ability to synthesize c-di-GMP in the absence of its cognate receptor LapD;
43 GcbC-LapD interaction enhances c-di-GMP synthesis by GcbC, likely mediated by the I-site of
44 GcbC. We further show evidence for a ligand-mediated mechanism of signaling specificity via
45 increased physical interaction of a DGC with its cognate receptor. We envision a scenario
46 wherein a "cloud" of weakly active DGCs can increase their activity by specific interaction with
47 their receptor in response to appropriate environmental signals, concomitantly boosting c-di-
48 GMP production, ligand-specific signaling and biofilm formation.

49

50 **Introduction.** For most bacteria, biofilm formation is a highly regulated event (1, 2). The
51 bacterial intracellular second messenger, cyclic dimeric GMP (c-di-GMP) controls biofilm
52 formation by regulating a diversity of biofilm-relevant outputs (3), including flagellar motility
53 (4), extracellular polysaccharide production (5, 6), adhesin localization (7), and transcriptional
54 control of pathways important for early biofilm formation (8). An important research theme in
55 the field has been understanding the mechanism(s) of c-di-GMP signaling-specificity in the
56 context of microbes that can have >50 proteins that make, degrade and bind this second
57 messenger.

58 Biofilm formation by *Pseudomonas fluorescens* Pf0-1 occurs when the adhesin LapA localizes to
59 the cell surface (9). LapA is maintained on the cell surface when the inner membrane protein
60 LapD binds c-di-GMP. The c-di-GMP-bound, inner membrane-localized LapD sequesters LapG,
61 thus this protease is unable to target the N-terminal cleavage site of LapA (10, 11). One

62 example of how c-di-GMP is specifically transferred to the LapD receptor is by physical
63 interaction with a diguanylate cyclase (DGC) (12). The DGC called GcbC has been shown to
64 physically interact with LapD utilizing a surface exposed α-helix of the GGDEF domain on GcbC
65 and a surface exposed α-helix of the EAL domain of LapD (12). We also demonstrated
66 previously that the I-site of GcbC contributes to the interaction of this enzyme with LapD (13).
67 This direct interaction model was proposed as one means to confer signaling specificity (12, 14).

68 GcbC is an inner membrane protein that contains a putative calcium channel chemotaxis
69 receptor (CACHE) domain N-terminal to its GGDEF domain; this CACHE domain is predicted to
70 reside in the periplasm. CACHE domains can be responsible for small ligand sensing (15). Many
71 signal transduction proteins, including DGCs and histidine kinases, contain CACHE domains,
72 which are involved in modulating these enzyme activities (16, 17, 18). GcbC, along with five
73 other DGCs encoded on the *P. fluorescens* Pf0-1 genome (Pfl01_1336, Pfl01_2295, Pfl01_2297,
74 Pfl01_3550, and Pfl01_3800), contain putative periplasmic CACHE domains located N-terminally
75 to their GGDEF domain, suggesting that these six DGCs are capable of sensing and responding
76 to small ligands. The predicted domain organization of three of these CACHE-containing
77 proteins, GcbC, Pfl01_2295, and Pfl01_2297, is shown in Figure 1A.

78 In this study, we analyze the putative CACHE domain of GcbC and identify two environmentally
79 relevant organic acids, including citrate, as a ligand for this DGC. We show citrate-enhanced
80 physical interaction of GcbC and LapD, and that this enhanced interaction promotes increased
81 c-di-GMP synthesis by GcbC, thereby promoting biofilm formation. We also describe another
82 example of such ligand-mediated enhancement of biofilm formation, suggesting the generality
83 of this mechanism. Furthermore, we show that GcbC has little propensity to synthesize c-di-

84 GMP in isolation; it is only in the presence of its receptor, LapD, that GcbC makes high levels of
85 c-di-GMP. We propose that the I-site of GcbC serves two roles beyond allosteric control of this
86 enzyme: promoting LapD-GcbC interaction and stabilizing the active conformation of GcbC in
87 this complex. Thus, we propose a mechanism whereby GcbC engagement with its receptor
88 LapD, which is enhanced by environmental cues, could serve as a general mechanism to confer
89 specificity to this complex signaling network.

90

91 **Results**

92 **Citrate-Mediated Biofilm Enhancement is Dependent on GcbC Activity.** Automated domain
93 annotation software predicts a CACHE domain in the periplasmic portion of GcbC (Figure 1A).
94 To identify small molecules that the CACHE domain of GcbC may bind, we performed a CLUSTAL
95 alignment of this amino acid sequence with CACHE domains of known structure (19). GcbC
96 showed the highest amino acid similarity to rpHK1S-Z16 (PDB ID: 3LIF) of *Rhodopseudomonas*
97 *palustris* with 31% identity (Fig. S1). When crystallized, the CACHE domain of rpHK1S-Z16 was
98 bound to citrate and methyl-2,4-pentanediol, two small ligands recruited from the
99 crystallization cocktail (19). Because ligand binding by CACHE domains has been shown to
100 activate the C-terminally fused histidine kinase (HK) and DGC domains (17, 18), we
101 hypothesized citrate may stimulate GcbC activity to enhance biofilm formation.

102 To test this idea, we compared the impact of citrate on biofilm formation in the wild type *P.*
103 *fluorescens* Pf0-1 and a *gcbC* mutant. In a wild-type (WT) background, a 50% increase in biofilm
104 formation was observed in the presence of citrate (Fig. 1B). However, citrate-mediated

105 enhancement of biofilm formation observed for the wild-type (WT) strain was abolished in the
106 *gcbC* mutant (Fig. 1B), suggesting that citrate-mediated enhancement of biofilm formation is
107 dependent on the presence of GcbC. Also, we found that increasing concentrations of citrate
108 further enhanced biofilm formation of *P. fluorescens* by up to ~100%. (Fig. S2A)

109 Next, we selected the CACHE domain-containing Pfl01_2295 and Pfl01_2297 proteins (Fig. 1A),
110 both of which interact with LapD (20), to serve as controls to determine if other CACHE
111 domains also respond to citrate to promote biofilm formation. For these studies, we used a *P.*
112 *fluorescens* Pf0-1 strain lacking four DGCs, referred to as Δ4DGC, which does not form a biofilm
113 under our laboratory conditions; this low c-di-GMP producing strain was previously used to
114 investigate c-di-GMP production by other *P. fluorescens* DGCs (21). The four DGCs deleted in
115 the Δ4DGC strain, identified previously, are *gcbA*, *gcbB*, *gcbC*, and *wspR* (21). Of the three
116 CACHE domain-containing DGCs expressed in the Δ4DGC mutant background (GcbC,
117 Pfl01_2295, and Pfl01_2297), only the strain expressing GcbC responded to citrate with
118 increased biofilm formation (Fig. 1C). DGC-mediated c-di-GMP synthesis typically requires an
119 intact GGDEF active-site motif and mutation of this motif to GGAAF in GcbC eliminates catalytic
120 activity; this GcbC (GGAAF) mutant variant was shown previously to be stably expressed at a
121 level equivalent to the WT protein (21). When GcbC-GGAAF mutant protein was expressed in
122 the Δ4DGC mutant background, biofilm formation was abolished and notably, citrate-mediated
123 biofilm formation was also abolished (Fig. 1C).

124 We further assessed the functionality of GcbC, Pfl01_2295, and Pfl01_2297 as active DGCs via
125 assaying their ability to stimulate increased production of the Pel polysaccharide using congo
126 red (CR) binding assay. Increased CR binding indicates increased production of the Pel

127 polysaccharide, which is mediated by increased c-di-GMP production, thus dark red colonies
128 indicate robust Pel production and white colonies indicate a lack of Pel production. Each DGC
129 was cloned into an expression plasmid, then electroporated into *P. aeruginosa* PA14 and grown
130 under inducing conditions with 0.1% arabinose. When GcbC and Pfl01_2295 are expressed from
131 a plasmid, CR binding of Pel polysaccharide was robustly stimulated compared to the vector
132 only control (pMQ72, Fig. S3). When Pfl01_2297 was expressed from a plasmid, CR binding of
133 Pel polysaccharide was, at best, weakly stimulated compared to the vector only control. As a
134 control, a mutant defective in production of the Pel polysaccharide (Δ*pelA*) showed little CR
135 binding (Fig. S3). These data indicate that Pfl01_2295 and Pfl01_2297 are likely functional DGCs,
136 a point addressed further below.

137 Importantly, citrate-enhanced biofilm formation is dependent on LapA (Fig. S2B), indicating that
138 citrate acts via the known LapD-LapG-LapA pathway. To further support a role for LapA in
139 citrate-stimulated biofilm formation, we used *P. fluorescens* Pf0-1 strains carrying a HA-tagged
140 LapA variant to detect the amount of LapA at the cell surface, as reported (7,10), as a function
141 of the presence of citrate. In a WT *P. fluorescens* strain, citrate caused a 159% increase in LapA
142 pixel density, which suggests a higher abundance of LapA at the cell surface in the presence of
143 citrate (Fig. 1D). Only when GcbC was present and catalytically active did citrate cause an
144 increase in cell surface-associated LapA (Fig. 1D). As a control, minimal levels of signal were
145 detected in a *P. fluorescens* strain lacking LapA, as expected. Also, there was no detectable
146 difference of the amount of LapA in whole cell lysate in the presence and absence of citrate in
147 WT *P. fluorescens* (Fig. S2C). Taken together, these data show that citrate-mediated stimulation

148 of biofilm formation by WT *P. fluorescens* Pf0-1 requires the active diguanylate cyclase GcbC
149 and is associated with enhanced cell-surface LapA.

150 Citrate also enhances growth of *P. fluorescens* (Fig. S2D), but as described below, this enhanced
151 growth is not the basis for the enhanced biofilm formation in the presence of citrate.
152 Interestingly, despite its ability to stimulate biofilm formation, citrate caused a ~100% increase
153 in swimming motility (Fig. S2E), perhaps via the ability of citrate to enhance growth of *P.*
154 *fluorescens*.

155

156 **The Putative Ligand-Binding Site of the CACHE Domain is Important for GcbC-Mediated**
157 **Biofilm Formation.** CACHE domains are ubiquitous, periplasmic, ligand-binding domains (15,
158 16). In a previous study, the RXYF motif was found to be the most conserved feature among the
159 characterized CACHE domains (19). A mutation of the RXYF motif of the CACHE domain of KinD,
160 a histidine kinase in *Bacillus subtilis*, caused this microbe to lose its ability to respond to root
161 exudates, and resulted in decreased biofilm formation on tomato roots compared to a WT
162 strain (17).

163 We first assessed whether citrate-enhanced biofilm formation was due to increased protein
164 expression level. We measured protein levels of a HA-tagged GcbC variant (expressed from a
165 plasmid from the studies shown in Figures 1C and 1D) in the presence and absence of citrate
166 and found that citrate did not affect the production and/or stability of GcbC (Fig. 2A). Analysis
167 of the pixel density of the bands +/- citrate revealed a ratio of 1.05$\pm$0.08, indicating no change
168 in GcbC protein level when the cells are grown with citrate.

169 We next sought to identify the putative site where citrate might bind to GcbC using the known
170 structures of CACHE domains (Fig. 2B, left; template PDB ID 3LIB). Like in the other CACHE
171 domains, the tyrosine residue of the RXYF motif of GcbC was predicted to point towards the
172 ligand-binding site (Fig. 2B, Fig. S4). Furthermore, based on the CACHE domain model of GcbC,
173 the amino acids R139, R162, and R172 were identified as candidates to shape the predicted
174 ligand-binding site (Fig. 2B, right). Based on the model, we predict that three arginine residues
175 can coordinate the three carboxylic acid groups of citrate (Fig. 2B, right). R139 is also part of the
176 RXYF motif. To probe whether these residues were involved in the citrate-mediated
177 enhancement of biofilm formation, each of the arginine residues forming the putative ligand-
178 binding site was mutated in GcbC and the mutant protein expressed from a plasmid introduced
179 into the Δ4DGC mutant background. Mutating R172 (R172A and R172E) resulted in loss of
180 stability of GcbC (Table S1), however GcbC-R139A, GcbC-R139E, and GcbC-R162A variants were
181 detected by Western blot, with GcbC-R139E variant present at approximately WT levels (Fig.
182 2C).

183 We next assessed whether the CACHE domain was required for citrate-enhanced biofilm
184 formation. The strain carrying GcbC-R139E variant, as well as the less stable GcbC-R139A and
185 GcbC-R162A alleles, did not show a significant enhancement of biofilm formation in the
186 presence of citrate (Fig. 2D). We further expanded our search for important conserved residues
187 within the CACHE domain that were predicted based on alignments with other CACHE domain
188 proteins, however the other twenty-seven mutant proteins we constructed were unstable
189 (Table S1). Together, our data indicate that the RXYF motif, and specifically R139 of the putative

190 citrate-binding arginine triad, is critical for GcbC-dependent, citrate-mediated enhancement of
191 biofilm formation.

192

193 **Selected Organic Acids Stimulate Biofilm Formation via GcbC**. We next sought to identify other
194 ligands that may be sensed by the CACHE domain of GcbC, given that some characterized
195 CACHE domains bind multiple ligands (19, 22). Based on the ability of the putative arginine triad
196 to bind the three carboxyl groups of citrate, we tested whether other organic acids (Fig. S5A),
197 including acetate (C2), pyruvate (C3), succinate (C4), fumarate (C4), α-ketoglutarate (C5) or
198 isocitrate (C6) could enhance biofilm formation in a GcbC-dependent manner. In both a WT *P.*
199 *fluorescens* strain and when GcbC is expressed in a Δ4DGC mutant strain, only isocitrate
200 significantly enhanced biofilm formation, and did so by 40% (Fig. S5B). Like citrate, isocitrate is a
201 C6 compound which contains three carboxyl groups (Fig. S5A). Also, isocitrate did not stimulate
202 biofilm formation by the strain carrying the GcbC-R139E variant (Fig. S5C), indicating that the
203 R139E variant was not responsive to citrate or isocitrate. Taken together, these data indicate
204 that the CACHE domain of GcbC likely binds citrate and isocitrate.

205

206 **Citrate-Mediated Interaction of GcbC with LapD Enhances Synthesis of c-di-GMP.** In our
207 published model, GcbC mediates biofilm formation by transferring c-di-GMP to LapD through
208 physical interaction, as demonstrated by both pull-down and bacterial two-hybrid assay (12).
209 We further showed that the LapD-GcbC interaction is mediated via the $\alpha5^{GGDEF}$ helix of GcbC
210 with the $\alpha2^{EAL}$ helix of LapD (12). This LapD-GcbC interaction also requires the I-site of GcbC

211 (13). We asked whether citrate might exert its effect of stimulating biofilm formation via
212 stabilization of the LapD-GcbC signaling complex. To test if citrate bolsters GcbC-LapD
213 interaction, we exploited the bacterial two-hybrid system used to initially demonstrate
214 interaction between these proteins (12). We did observe a modest but significant enhancement
215 of LapD-GcbC interaction in the presence of citrate (Fig. 3A). No such enhancement was
216 observed for the control interactions: LapD-Pfl01_2295, or GcbC with a dual domain protein
217 (Pfl01_0192; this protein has cytoplasmic GGDEF and EAL domains similar to LapD) or a
218 phosphodiesterase (Pfl01_2920, Fig. 3A). Citrate also did not enhance GcbC-GcbC dimerization
219 (Fig. 3A). Further, the catalytically inactive variant of GcbC still showed citrate-stimulated
220 interaction similar to WT GcbC (Fig. 3A). Finally, the GcbC-R139E mutant variant did not show a
221 significant, citrate-mediated increased interaction (Fig. 3A), consistent with our data above that
222 this residue is required for citrate-mediated enhancement of biofilm formation (Fig. 2D).

223 We further explored whether citrate could also enhance the diguanylate cyclase activity of
224 GcbC. We used the bacterial two-hybrid (B2H) plasmids and strains to express GcbC and LapD
225 outside of their native context, and to better focus on how the interaction of these two
226 proteins might specifically impact GcbC's activity. The activity of GcbC was assessed by
227 measuring the level of c-di-GMP extracted from the *E. coli* strains that carry plasmids containing
228 the indicated genes (Fig. 3B). The level of c-di-GMP measured in the *E. coli* strain carrying the
229 vector control was <0.5 pmol c-di-GMP/mg dry weight of bacteria (Fig. 3B). This low
230 background of c-di-GMP provided a useful tool to measure differences in c-di-GMP levels
231 derived from GcbC in the presence and absence of citrate and the LapD receptor.

232 GcbC alone did not synthesize levels of c-di-GMP above background and citrate did not
233 promote c-di-GMP production using three different strains wherein only GcbC was expressed
234 (Fig. 3B; pMQ72-GcbC, pKNT25-GcbC + pUT18, pKNT25-GcbC + pUT18-GcbC), a finding
235 consistent with a previous study in which low levels of c-di-GMP synthesis by GcbC were
236 detected (21). Co-expression of GcbC with LapD resulted in ~4 pmol c-di-GMP/mg dry weight,
237 an ~8-fold increase above the control level, and the level of c-di-GMP was further, significantly
238 increased to ~7 pmol c-di-GMP/mg dry weight upon addition of citrate (Fig. 3B). This finding has
239 two important implications. First, GcbC activity is apparently stimulated when engaging its
240 cognate LapD receptor, suggesting a mechanism for specific signaling between GcbC and LapD.
241 Second, enhanced interaction of GcbC and LapD upon addition of citrate further enhances c-di-
242 GMP production by GcbC.

243 Modest amounts of c-di-GMP catalysis occurred when the catalytically inactive GcbC variant
244 was coexpressed with LapD, but the addition of citrate did not significantly enhance the level of
245 c-di-GMP (Fig. 3B). Additionally, Pfl01_0192, a dual GGDEF-EAL domain protein with a
246 cytoplasmic domain organization similar to LapD, which was shown to interact weakly with
247 GcbC (Fig. 3A), produced levels of c-di-GMP in the presence of GcbC that were above
248 background but did not increase with added citrate (Fig. 3B).

249 We investigated the impact of the GcbC-R139E CACHE-domain mutation on citrate-mediated
250 LapD-GcbC interaction and c-di-GMP synthesis. While the GcbC-R139E/LapD interaction was
251 equivalent to the interaction between LapD and the wild-type GcbC, citrate-enhanced
252 interaction of GcbC-R139E-LapD showed a small, but non-significant increase (Fig. 3A). This
253 finding was consistent with the data above (Fig. 2D), showing that the GcbC-R139E mutant was

254 still capable of promoting biofilm formation in the Δ4DGC background, but biofilm formation
255 was not enhanced by the addition of citrate. Furthermore, and consistent with the bacterial
256 two-hybrid data, basal c-di-GMP levels were not affected by the GcbC-R139E mutant variant
257 compared to the WT GcbC when coexpressed with LapD (Fig. 3B). Importantly, there was no
258 significant increase in c-di-GMP level when the GcbC-R139E mutant variant was coexpressed
259 with LapD in the presence of citrate (Fig. 3B). Thus, our data indicate that LapD-GcbC
260 interaction enhances c-di-GMP production, and the addition of citrate stimulates both
261 interaction of LapD-GcbC and c-di-GMP synthesis, likely via the CACHE domain of GcbC.

262 When GcbC is removed from its native context and expressed in a heterogenous system, this
263 enzyme did not produce levels of c-di-GMP above background (Fig. 3B). This finding suggested
264 that GcbC might be inactive until it engages its cognate receptor LapD. To test this idea, we
265 assessed c-di-GMP production by I-site mutant variants of this enzyme expressed in the B2H *E.*
266 *coli* strain. The canonical role of the I-site is to reduce GcbC catalytic activity when c-di-GMP is
267 bound, and we previously identified two different mutants of GcbC in our near the I-site, R363E
268 and R366E, which greatly enhanced biofilm formation and c-di-GMP levels when expressed in *P.*
269 *fluorescens* (13). These I-site-proximal mutations also reduced interaction with LapD (13). When
270 expressed on its own, the GcbC-R366E I-site mutant was not able to synthesize c-di-GMP levels
271 above background (Fig. 3B). We observe a similar phenotype for the R363E mutant; R363
272 stabilizes the GGDEF domains as they come together in a GGDEF dimer with c-di-GMP at the I-
273 site. Only when LapD was present were high levels of c-di-GMP produced, with GcbC-R363E-
274 expressing strain synthesizing ~60pmol c-di-GMP/mg dry weight and GcbC-R366E-expressing
275 strain synthesizing ~20pmol c-di-GMP/mg dry weight (Fig. 3B). These levels of c-di-GMP were

276 significantly higher than the level detected for wild-type GcbC, and citrate did not further
277 enhance c-di-GMP production for either I-site mutant (Fig. 3B). These data strongly support the
278 model that GcbC has little or no activity until this enzyme engages its cognate receptor.

279

280 **A Conserved Mechanism of Signaling Specificity.** We next explored if the mechanism we
281 defined for GcbC-LapD interactions might apply to any of the other 20 DGCs in *P. fluorescens*.
282 We found that LapD is a central hub of DGC interaction; LapD interacts with nine different DGCs
283 in a pairwise bacterial two-hybrid assay (Fig. 4A,C). Included among the nine DGCs that interact
284 with LapD are the CACHE domain-containing DGCs Pfl01_2295 and Pfl01_2297, and the
285 putative SadC homolog, Pfl01_4451 (Fig. 4A). SadC is a DGC identified for its role in the early
286 stages of biofilm formation by *P. aeruginosa* (23, 24), and the Δ*sadC* mutant of *P. aeruginosa*
287 shows approximately a 50% reduction of global, cellular c-di-GMP levels compared to WT *P.*
288 *aeruginosa* PA14 (24).

289 Given that there are nine DGCs that interact with LapD, we hypothesized that each of the nine
290 DGCs may compete with one another to interact with LapD. To test this model, we
291 overexpressed WT GcbC and the catalytically inactive variant of GcbC in a WT *P. fluorescens*
292 strain. When the catalytically inactive GcbC variant was overexpressed, biofilm formation was
293 significantly reduced by ~20% (Fig. 4B), indicating that the catalytically inactive variant of GcbC
294 is displaying a dominant negative phenotype, a finding consistent with our competition
295 hypothesis. As a control, when WT GcbC was overexpressed, biofilm formation was significantly
296 enhanced, as expected (Fig. 4B).

297 We next explored if the ligand-mediated signaling specificity mechanism is conserved among
298 other CACHE-containing DGCs. We focused on Pfl01_2295 given that this DGC shows similar
299 levels of interaction with LapD as was observed for GcbC (Fig. 4C), and the likely robust c-di-
300 GMP synthesis activity as indicated by the robust CR binding observed when Pfl01_2295 was
301 expressed from a plasmid in *P. aeruginosa* (Fig. S3). Also, the CACHE domain of Pfl01_2295
302 contains the conserved RXYF motif (Fig. S6), and contains two of the three arginine residues
303 that comprise the putative ligand binding site of the CACHE domain of GcbC. Thus, we
304 predicted that Pfl01_2295 would sense ligands that are similar to, but different from, citrate. To
305 test this idea, we expressed Pfl01_2295 in the Δ4DGC mutant background and performed a
306 biofilm assay with medium supplemented with exogenous acetate, pyruvate, succinate,
307 fumarate, or isocitrate. Citrate was shown not to stimulate biofilm formation through
308 Pfl01_2295 nor enhance LapD – Pfl01_2295 interaction as measured using the bacterial two-
309 hybrid assay (Fig. 1C, Fig. 3A).

310 Succinate significantly enhanced biofilm formation in the presence of Pfl01_2295 and also
311 significantly enhanced interaction with LapD (Fig. 5A). Thus, this finding mirrored what we
312 observed for citrate and isocitrate with GcbC. Interestingly, acetate significantly stimulated
313 Pfl01_2295-dependent biofilm formation, but did not stimulate interaction with LapD (Fig. 5B),
314 perhaps indicating that acetate stimulates Pfl01_2295 activity but not the ability of this DGC to
315 interact with its receptor. Pyruvate, fumarate, and isocitrate had no effect in stimulating biofilm
316 formation in a Δ4DGC mutant background with Pfl01_2295 expressed from a plasmid (Fig. S7).

317

318 **Discussion**. A key open question relating to c-di-GMP signaling is how specificity of a particular
319 output can be mediated in the context of up to dozens of enzymes or receptors making,
320 breaking and binding this dinucleotide second messenger. Here, our data suggest two related
321 mechanisms for controlling output specificity. First, GcbC shows little activity unless it is co-
322 expressed with its receptor. Furthermore, we show that an extracellular ligand can modulate
323 the activity of a GcbC and does so via promoting interaction of the DGC with its cognate
324 receptor. Our data are consistent with the model that citrate or isocitrate binding to the CACHE
325 domain of GcbC enhances interaction with LapD. We propose the increased interaction
326 between GcbC and LapD to have two important consequences: stabilization of a complex that
327 allows direct transfer of the GcbC-generated c-di-GMP signal to the LapD receptor, and equally
328 importantly, activation of the DGC activity of GcbC. Our data suggest that for at least this DGC,
329 GcbC must be in complex with its receptor to be activated. An additional boost in cyclic
330 nucleotide production was measured when citrate or isocitrate was added to the medium in a
331 strain co-expressing GcbC and LapD, indicating that the enhanced GcbC-LapD interaction also
332 enhanced DGC activity. Furthermore, recent work from the Sondermann lab (25) identified a
333 LapD dimer-of-dimers as a c-di-GMP- and LapG-bound state, which could serve as an
334 interaction platform or "receptor basket" for GcbC, thereby forming a large LapD-LapG-GcbC-c-
335 di-GMP signaling complex (Fig. 5C). Our data adds to this model a ligand-based mechanism to
336 enhance the interaction between GcbC and LapD, and thus signaling specificity in the context of
337 a large signaling network.

338 We suggest a possible mechanism whereby c-di-GMP production by GcbC is promoted when
339 this DGC is in complex with LapD. Our data here suggest that as a baseline condition, GcbC

340 activity is low, a finding consistent with a previous study in which low levels of c-di-GMP
341 synthesis by GcbC were detected (21). Surprisingly, we detected little c-di-GMP production by
342 two different I-site-proximal variants of GcbC when this enzyme was expressed on its own,
343 consistent with the idea that this enzyme is likely inactive when not engaging its receptor. How
344 then does the GcbC-LapD interaction stimulate GcbC activity? We reported previously the
345 somewhat unexpected finding that the I-site of GcbC is required for full LapD-GcbC interaction
346 (13). Based in part on this finding, we propose that the I-site of this diguanylate cyclase (Fig. 5C,
347 orange star in GcbC) may engage LapD (rather than c-di-GMP) to help promote stabilization of
348 the active form of the GcbC. In this model, we propose that it is only when local c-di-GMP levels
349 become very high that GcbC is driven towards the inactive state via I-site binding by the
350 dinucleotide. The addition of citrate may further stabilize the active conformation of GcbC,
351 both by enhancing GcbC-LapD interaction via the GcbC I-site (and likely other interactions (13))
352 and promoting higher levels of c-di-GMP production.

353 We have identified two C6, three carboxyl group-containing organic acids, citrate and isocitrate,
354 as potential ligands that bind to GcbC via its CACHE domain. There are an abundance of CACHE
355 domains present as components of signal transduction proteins (16), including proteins
356 involved in c-di-GMP signaling, and yet, the role of CACHE domains in regulating DGC activity is
357 poorly understood. Our data show that citrate and isocitrate are likely ligands for the CACHE
358 domain associated with GcbC. *P. fluorescens*, a plant-growth promoting microbe, forms biofilms
359 on tomato roots; root exudates contain a high abundance of low molecular weight organic
360 acids, including citrate (26, 27, 28). We suggest that many compounds found in root exudates,

361 including additional organic acids, sugars, and metals, may be used as signals by *P. fluorescens*
362 to promote biofilm formation.

363 As we have shown here, GcbC appears to sense citrate and isocitrate, but not a variety of other
364 structurally related molecules. It is possible that the CACHE domain of GcbC responds to
365 additional signals. For example, in *P. syringe* pv. *actinidiae*, the CACHE domain PscD (PDB ID:
366 5G4Z) binds glycolate, acetate, propionate, and pyruvate (22), indicating that CACHE domains
367 allow for some promiscuity in their binding of ligands. GcbC has been shown to be part of a
368 large signaling network, interacting with a phosphodiesterase and multiple dual domain
369 containing proteins (20), thus also opening the possibility that different ligands sensed via the
370 CACHE domain of GcbC could dictate which proteins interact with this DGC.

371 We showed that while GcbC responds to exogenous citrate and isocitrate, other CACHE
372 domain-containing DGCs do not respond to these organic acids. We identified the RXYF motif
373 as important for signal sensing by GcbC. Furthermore, the residue R162, but not R172, is
374 conserved among the CACHE domains of GcbC, Pfl01_2295, Pfl01_2297, and Pfl01_3800 (Fig.
375 S6), thus this variation in sequence likely speaks to the inability of these other DGCs to respond
376 to the same ligands as GcbC. Consistent with the idea that these other CACHE domains bind
377 other signals, we have identified acetate and succinate as potential ligands that are sensed via
378 the CACHE domain of Pfl01_2295. Only succinate enhanced Pfl01_2295-LapD interaction, while
379 acetate promoted Pfl01_2295-dependent biofilm formation but did not enhance LapD
380 interaction. Thus, ligand binding may exert a variety of effects on target proteins. Such a
381 finding may not be surprising in the context of this complex c-di-GMP network, as multiple
382 pathways contribute to biofilm formation and many DGCs have multiple interaction partners

383 (20). Additional work is required to identify all of the ligands that impact the c-di-GMP network
384 in this organism.

385 Together, our data indicate that extracellular ligands, via their ability to impact protein-protein
386 interactions and/or DGC activity, can modulate c-di-GMP signaling specificity. We think it is
387 unlikely that all nine DGCs shown to interact with LapD do so simultaneously and with high
388 affinity. Rather, we envision a scenario wherein a "cloud" of DGCs with low activity perhaps
389 weakly interact with their receptor(s); a specific DGC-receptor interaction may increase in
390 response to appropriate environmental signals, concomitantly boosting c-di-GMP production,
391 ligand-specific signaling and biofilm formation. Overall, our work provides insight into a ligand-
392 mediated mechanism conferring signaling specificity within a complex network of enzymes and
393 receptors that make, break, and bind c-di-GMP. Given the large number of ligand-binding
394 domains associated with c-di-GMP-metabolizing proteins, the data presented here could
395 represent a general means of regulating c-di-GMP-controlled outputs by enhancing specific
396 interactions between c-di-GMP-metabolizing enzymes and their effectors.

397

398 **Material and Methods**

399 **Strains and Media.** Bacterial strains used in this study are listed in Table S2, and were cultured
400 and maintained in lysogeny broth (LB) or on 1.5% agar LB plates. *P. fluorescens* was grown at
401 30°C and *P. aeruginosa* and *E. coli* was grown at 37°C. *E. coli* S17-1-λ-pir was used for
402 maintenance and transfer of plasmids. *Saccharomyces cerevisiae* strain InvSc1 was used for
403 plasmid modification as described previously (29, 30). K10T-1 medium was prepared as

404 described previously (31). Sodium citrate was added to 1.5% agar LB plates and K10T-1 media
405 to a final concentration of 13.6 mM (0.4% wt/vol) for all the experiments described. All organic
406 acids were set at 0.4% wt/ vol and the following concentrations were set as indicated: sodium
407 acetate (29.4mM), pyruvic acid (45.4mM), sodium succinate (14.8mM), sodium fumarate
408 (25.0mM), α-ketoglutarate (27.4mM), and isocitrate (15.5mM). The following antibiotics were
409 used as indicated: gentamycin (15µg/mL for *E. coli*, 30µg/mL for *P. fluorescens* and *P.*
410 *aeruginosa*), kanamycin (50µg/mL for *E. coli*), and carbenicillin (50µg/mL for *E. coli*).

411 **Biofilm Assay.** Biofilm assays were performed as described previously (1). *P. fluorescens* Pf0-1
412 strains were incubated in K10T-1 minimal medium with and without 0.4% organic acid, as
413 indicated, for 6 hours at 30°C. Biofilms were stained with 0.1% crystal violet, washed with
414 water and then solubilized with a 45% methanol, 45% dH_2O, and 10% glacial acetic acid
415 solution. The optical density (OD) of the solubilized crystal violet solution was measured at 550
416 nm to determine the amount of biofilm formed.

417 **Dot Blot for LapA Localization Assay.** Localization of LapA to the cells surface was measured
418 using a HA-tagged LapA variant integrated into the chromosome of *P. fluorescens* as described
419 previously with slight modification (7, 10, 32). Bacterial cultures were grown overnight in LB
420 and then subcultured into 5mL K10T-1 at a 1:50 dilution for 6 hours at 30°C. To test how
421 sodium citrate effected LapA localization to the cell surface, sodium citrate was added at the
422 beginning of the 6-hour subculturing period. After 6 hours of incubation, cells were normalized
423 to the lowest OD value, washed twice in K10T-1, and 5µl aliquots were spotted onto a
424 nitrocellulose membrane. Once dried, HA-tagged LapA was probed for by Western blot analysis.

425 **Bacterial Two-Hybrid Assay.** Bacterial two-hybrid (B2H) assays were performed using *E. coli*
426 BTH101 cells based on a previously described system (33). Briefly, ~100 ng of each bacterial
427 two hybrid plasmid was cotransformed into *E. coli* BTH101 by electroporation. *E. coli* BTH101
428 cells were incubated on LB agar supplemented with 50µg/mL kanamycin, 50µg/mL carbenicillin,
429 and 0.5mM isopropyl β-D-1-thiogalactopyranoside (IPTG) for 24 hours at 30°C. At 24 hours,
430 either β-galactosidase or c-di-GMP levels were quantified as described below. β-galactosidase
431 assays were performed as exactly described previously (12) to quantify the extent of protein-
432 protein interaction. β-galactosidase levels are presented in Miller Units.

433 **c-di-GMP Quantification Assay.** c-di-GMP was extracted from *E. coli* BTH101 cells after
434 incubation on LB agar plates at 30°C for 24 hours. The cells were scraped from the plate surface
435 with 1 mL of dH_2O, then pelleted and resuspended in 0.250 mL nucleotide extraction buffer
436 (40% methanol, 40% acetonitrile, 20% dH_2O, and 0.1N formic acid), followed by incubation at -
437 20°C for 1 hour. Cells were pelleted again and the reaction was neutralized by transfer of 0.2
438 ml nucleotide extract to 8µl of 15% NH_4CO_3. Nucleotide extracts were vacuum-dried and
439 resuspended in 0.2 mL HPLC grade H_2O. c-di-GMP concentration was analyzed by liquid
440 chromatography-mass spectrometry and compared to a standard curve of known c-di-GMP
441 concentration, as reported (12). The mols of c-di-GMP were normalized to the dry weight of the
442 cell pellet from which the nucleotides were extracted.

443 **Congo Red Binding Assay**

444 Assessment of DGC activity using the congo red binding assays was performed as described
445 previously (12).

446 **Swim Motility Assay**

447 Swim motility assays were performed as described previously (21). K10T-1 plates containing
448 0.35% agar were prepared by adding filter-sterilized K10T-1 media to an autoclaved, molten
449 agar solution and plates were solidified for 3 hours. Overnight cultures were normalized to the
450 lowest OD value and washed twice in K10T-1 medium. A 2-200µl pipette micropipette tip was
451 used to inoculate each plate. A sterile pipette tip was dipped into each strain and plunged
452 halfway into the swim agar plate. Plates were incubated at 30°C for ~30 hours and plates were
453 photographed. The swim area was calculated using ImageJ software.

454 **Growth Curve Assay**

455 The amount of growth of *P. fluorescens* in the presence and absence of citrate was measured.
456 Bacterial cultures were grown overnight in liquid LB and then subcultured in 5mL K10T-1 with
457 and without 0.4% citrate at a 1:50 ratio for 6 hours at 30°C. Every two hours, the OD of the
458 bacterial culture was measured at 600nm to determine the amount of growth that occurred.

459

460 **Acknowledgement.** We thank members of the lab for helpful discussions, the reviewers for
461 their helpful comments, and Tom Hampton for assistance with statistical analysis. This work
462 was supported by the NIH via grant R01GM123609 (to H.S. and G.A.O.) and P20 RR030360.

463

464

465 **Literature Cited.**

466 1. O'Toole GA, Kolter R (1998) Initiation of biofilm formation in *Pseudomonas fluorescens*
467 WCS365 proceeds via multiple, convergent signaling pathways: A genetic analysis. *Mol*
468 *Microbiol* 28: 449-461.
469 2. Pruss BM, Besemann C, Denton A, Wolfe AJ (2006) A complex transcription network
470 controls the early stages of biofilm development by *Escherichia coli*. *J Bacteriol* 188(11):
471 3731-3739.
472 3. Römling U, Gomelsky M, Galperin MY (2005) c-di-GMP: The dawning of a novel bacterial
473 signaling system. *Mol Microbiol* 57(3): 629-639.
474 4. Baker AE, Diepold A, Kuchma SL, Scott JE, Ha DG, Orazi G, Armitage JP, O'Toole GA (2016)
475 A PilZ domain protein FlgZ mediates cyclic-di-GMP-dependent swarming motility control
476 in *Pseudomonas aeruginosa*. *J Bacteriol* 198(13): 1837-1846.
477 5. Ross P, Weinhouse H, Aloni Y, Michaeli D, Weinberger-Ohana P, Mayer R, Braun S, de
478 Vroom E, van der Marel GA, van Boom JH, Benziman M (1987) Regulation of cellulose
479 synthesis in *Acetobacter xylinum* by cyclic diguanlyic acid. *Nature* 325(6101): 279-281.
480 6. Merrit JH, Brothers KM, Kuchma SL, O'Toole HA (2007) SadC reciprocally influences
481 biofilm formation and swarming motility via modulation of exopolysaccharide production
482 and flagellar function. *J Bacteriol* 189(22): 8154-8164.
483 7. Monds RD, Newell PD, Gross RH, O'Toole GA (2007) Phosphate-dependent modulation of
484 c-di-GMP levels regulates *Pseudomonas fluorescens* Pf0-1 biofilm formation by controlling
485 secretion of the adhesin LapA. *Mol Microbiol* 63(3): 659-679.

486 8. Martínez-Gil M, Ramos-González MI, Espinosa-Urgel M (2014) Roles of cyclic di-GMP and
487 the Gac system in transcriptional control of the genes coding for *Pseudomonas putida*
488 adhesins LapA and LapF. *J Bacteriol* 196(8): 1484-1495.
489 9. Hinsa SM, Espinosa-Urgel M, Ramos JL, O'Toole HA (2003) Transition from reversible to
490 irreversible attachment during biofilm formation by *Pseudomonas fluorescens* WCS365
491 requires an ABC transporter and a large secreted protein. *Mol Microbiol* 49: 905-918.
492 10. Newell PD, Monds RD, O'Toole GA (2009) LapD is a bis-(3'-5')-cyclic dimeric GMP-binding
493 protein that regulates surface attachment by *Pseudomonas fluorescens* Pf0-1. *Proc Natl*
494 *Acad Sci USA* 106(9): 3461-3466.
495 11. Navarro MV, Newell PD, Krasteva PV, Chatterjee D, Madden DR, O'Toole GA, Sondermann
496 HA (2011) Structural basis for c-di-GMP-mediated inside-out signaling controlling
497 periplasmic proteolysis. *PLoS Biol* 9(2): e1000588. doi: 10.1371.
498 12. Dahlstrom KM, Giglio KM, Collins AJ, Sondermann H, O'Toole GA (2015) Contribution of
499 physical interactions to signaling specificity between a diguanylate cyclase and its effector.
500 *mBio* 6(6):e01978-15. doi:10.1128/mBio.01978-15.
501 13. Dahlstrom KM, Gilgio KM, Sondermann H, O'Toole GA (2016) The inhibitory site of a
502 diguanylate cyclase is a necessary element for interaction and signaling with an effector
503 protein. *J Bacteriol* 198(11): 1595-1603.
504 14. Dahlstrom KM, O'Toole GA (2017) A symphony of cyclases: specificity in diguanylate
505 cyclase signaling. *Annu Rev Microbiol* 71: 179-195.

506 15. Anantharamn V, Aravind L (2000) Cache – a signaling domain common to animal Ca(2+)-
507 channel subunits and a class of prokaryotic chemotaxis receptors. *Trends Biochem Sci*
508 25(11): 535-537.
509 16. Upadhyay AA, Fleetwood AD, Adebali O, Finn RD, Zhulin IB (2016) Cache domains that are
510 homologous to, but different from PAS domains comprise the largest superfamily of
511 extracellular sensors in prokaryotes. *PLoS Comput Biol* 12(4): e1004862. doi:
512 10.1371/journal.pcbi.1004862.
513 17. Chen Y, Cao S, Chai Y, Clardy J, Kolter R, Guo JH, Losick R (2012) A *Bacillus subtilis* sensor
514 kinase involved in triggering biofilm formation on the roots of tomato plants. *Mol*
515 *Microbiol* 85(3): 418-430.
516 18. Mills E, Peterson E, Kulasekara BR, Miller SI (2015) A direct screen for c-di-GMP
517 modulators reveals a *Salmonella typhimurium* periplasmic L-arginine-sensing pathway. *Sci*
518 *Signal* 8(380): ra57. doi: 10.1126/scisignal.aaa1796.
519 19. Zhang Z, Hendrickson WA (2010) Structural characterization of the predominant family of
520 histidine kinase sensor domains. *J Mol Biol* 400(3): 335-353.
521 20. Dahlstrom KM, Collins AJ, Doing G, Taroni JN, Gauvin TJ, Greene CS, Hogan DA, O'Toole GA
522 (2018) A multimodal strategy used by a large c-di-GMP network. *J Bacteriol*.
523 doi:10.1128/JB.00703-00717.
524 21. Newell PD, Yoshioka S, Hvorecny KL, Monds RD, O'Toole GA (2011) Systematic analysis of
525 diguanylate cyclases that promote biofilm formation by *Pseudomonas fluorescens* Pf0-1. *J*
526 *Bacteriol* 193(18): 4685-4698.

527 22. Brewster JL, McKellar JL, Finn TJ, Newman J, Peats TS, Gerth ML (2016) Structural basis for
528 ligand recognition by a Cache chemosensory domain that mediates carboxylate sensing in
529 *Pseudomonas syringae*. *Sci Rep* 6:35198. doi: 10.1038/srep35198.
530 23. Merritt JH, Brothers KM, Kuchma SL, O'Toole GA (2007) SadC reciprocally influences
531 biofilm formation and swarming motility via modulation of exopolysaccharide production
532 and flagellar function. *J Bacteriol* 189(22): 8154-8164.
533 24. Merritt JH, Ha DG, Cowles KN, Lu W, Morales DK, Rabinowitz J, Gitai Z, O'Toole GA (2010)
534 Specific control of *Pseudomonas aeruginosa* surface-associated behaviors by two c-di-
535 GMP diguanylate cyclases. *Mbio* 1(4): e00183-10. doi:10.1128/mBio. 00183-10.
536 25. Cooley RB, O'Donnell JP, Sondermann H (2016) Coincidence detection and bi-directional
537 transmembrane signaling control a bacterial second messenger receptor. *Elife* 5: e21848
538 doi: 10.7554/eLife.21848.
539 26. Haas D, Défago G (2005) Biological control of soil-borne pathogens by fluorescent
540 pseudomonads. *Nat Rev Microbiol* 3(4): 307-319.
541 27. Jones DL (1998) Organic acids in the rhizosphere – a critical review. *Plant Soil* 205: 25-44.
542 28. de Weert S, Vermeiren H, Mulders IH, Kuiper I, Hendrickx N, Bloemberg GV, Vanderleyden
543 J, De Mot R, Lugtenberg BJ (2002) Flagella-driven chemotaxis towards exudate
544 components is an important trait for tomato root colonization by *Pseudomonas*
545 *fluorescens*. *Mol Plant Microbe Interact* 15(11): 1173-1180.
546 29. Shanks RMA, Calazza NC, Hinsa SM, Toutain CM, O'Toole GA (2006) *Saccharomyces*
547 *cerevisiae*-based molecular tool kit for manipulation of gram-negative bacterial genes.
548 *Appl Environ Microbiol* 72(7): 5027-5036.

549 30. Bascom-Slack CA, Dawson D (1998) A physical assay for detection of early meiotic
550 recombination intermediates in *Saccharomyces cerevisiae*. *Mol Gen Genet* 258: 512-520.
551 31. Monds RD, Newell PD, Schwartzman JA, O'Toole GA (2006) Conservation of the Pho
552 regulon in *Pseudomonas fluorescens* Pf0-1. *Appl Environ Microbiol* 72(3): 1910-1924.
553 32. Newell PD, Boyd CD, Sodermann H, O'Toole GA (2011) A c-di-GMP effector system control
554 cell adhesion by inside-out signaling and surface protein cleavage. *PloS Biol* 9(2):
555 e1000587. doi: 10.1371/journal.pbio.1000587.
556 33. Karimova G, Pidoux J, Ullmann A, Ladant D (1998) A bacterial two-hybrid system based on
557 a reconstituted signal transduction pathway. *Proc Natl Acad Sci USA* 95: 5752-5756.
558 34. Shultz J, Milpetz F, Bork P, Ponting CP (1998) SMART, a simple modular architecture
559 research tool: Identification of signaling domains. *Proc Natl Acad Sci USA* 95: 5857-5864.
560 35. Ulrich LE, Zhulin IB (2010) The MiST2 database: a comprehensive genomics resource on
561 microbial signal transduction. *Nucleic Acids Res* 38: D401-407 doi:10.1093/nar/gkp940.
562 36. R Core Team (2016) R: A language and environment for statistical computing. R
563 Foundation for Statistical Computing, Vienna, Austria. URL https://www.R-project.org/.

564

565 **Figure Legends**

566 **Fig. 1. Citrate stimulates biofilm formation via GcbC.** (A) Predicted domain organization of
567 GcbC, Pfl01_2295, and Pfl01_2297 as predicted by SMART (34). The domains are indicated in
568 each block. TM = transmembrane domain. Analysis of Pfl01_2295 by MiST2 (35) predicts a
569 second transmembrane domain. (B) Biofilm formation by WT *P. fluorescens* and the Δ*gcbC*
570 mutant in the presence and absence of 0.4% citrate (n = 3; ± SD). (C) Biofilm formation by the
571 indicated strains +/- citrate. In this panel, the Δ4DGC mutant background is used, with the WT
572 GcbC and the catalytically inactive variant (GGAAF) introduced into this mutant on plasmids.
573 Pfl01_2297 and Pfl01_2295 are two other CACHE-domain containing diguanylate cyclases in *P.*
574 *fluorescens*, expressed from the same vector backbone, that serve as controls. (D)
575 Quantification of cell-surface levels of LapA in the presence and absence of 0.4% citrate.
576 Representative blots are shown. For panels B, C, and D, the values shown are an average of 3
577 replicates (± SD); horizontal black bars indicate a P value of <0.05 (*), <0.01 (**), or <0.001 (***)
578 with a student's t-test compared to the condition without citrate.

579 **Fig. 2. Effects of CACHE domain mutations on biofilm formation.** (A) Western blot to assess the
580 level of GcbC-HA expressed from a plasmid in the presence and absence of citrate. This is the
581 GcbC-HA-expressing plasmid used in Figure 1. (B) Homology model of the CACHE domain of
582 GcbC based on rpHK1S-Z16 (PDB ID: 3LIF) and vpHK1S-Z8 (PDB ID: 3LID) (see Figure S1 and S4)
583 to identify the putative ligand-binding site. (C) Western blot assessment of the relative stability
584 of GcbC-R139A-HA, GcbC-R139E-HA and GcbC-R162A-HA mutant proteins compared to the WT
585 GcbC. These proteins were all expressed in Δ4DGC mutant *P. fluorescens* strain. (D)
586 Quantitative analysis of biofilm formation by strains expressing the indicated CACHE domain

587 mutants in the presence and absence of citrate. For panels A and E, data shown is the average
588 of three replicates (± SD); horizontal black bars indicate a P value of either <0.05 (*) or <0.001
589 (***) with a student's t-test comparing each strain without citrate versus with added citrate. ns,
590 not significant.

591 **Fig. 3. Citrate-mediated biofilm enhancement.** (A) The effect of citrate on interaction with the
592 indicated proteins is compared by the B2H assay, and expressed as Miller Units. Pfl01_2295 =
593 CACHE domain-containing DGC; Pfl01_0192 = GGDEF and EAL domain-containing protein;
594 Pfl01_2920 = EAL domain-containing protein. Briefly, the proteins of interest fused to two
595 halves of the catalytic domain of an adenylate cyclase from *Bordetella pertussis* (T25 and T18)
596 are transformed into *E. coli* BTH101 cells (33). Plasmids pKNT25 and pUT18 are the vector-only
597 controls. If the two proteins interact, the adenylate cyclase activity is reconstituted, promoting
598 cAMP synthesis, which in turn activates transcription of the *lacZ* gene and increases production
599 of its gene product. The β-galactosidase activity is assessed using ortho-nitrophenyl-β-
600 galactoside (ONPG) as a substrate, which serves as a measure of the degree of interaction (33).
601 Citrate did not enhance interaction of the vectors or of the positive control (GCN4 leucine
602 zipper protein). Citrate only enhanced the interaction between LapD and GcbC. The effect of
603 catalytic activity of GcbC on interaction with LapD was compared in the presence and absence
604 of 0.4% citrate. Mutation of the putative citrate-binding pocket in the CACHE domain of GcbC
605 (GcbC-R139E) resulted in the loss of citrate-stimulated GcbC-LapD interaction. (B) The B2H
606 assay strains were used to measure the effects of citrate on c-di-GMP synthesis by GcbC.
607 Plasmids were cotransformed as indicated into *E. coli* BTH101. After 24 hours of incubation at
608 30°C, nucleotides were extracted. C-di-GMP production in *E. coli* BTH101 was determined for

609 strains producing the indicated proteins. Only co-expression of LapD and GcbC showed
610 appreciable accumulation of c-di-GMP, which was significantly stimulated by added citrate. For
611 panels A and B, all experiments were performed in triplicate (± SD), with an indicated P value of
612 either <0.05 (*) or <0.01 (**) with a student's t-test comparing each strain without versus with
613 citrate. ns, not significant. For panel B, GcbC-LapD and GcbC R139E-LapD interactions are
614 represented by six biological replicates instead of three.

615 **Fig. 4. LapD interacts with multiple DGCs**. (A) Interaction map of DGCs that showed a
616 significant level of interaction with LapD by 24 hours, as compared to the negative control, by
617 B2H assay. Data that served as the basis for this model is shown in Figure 4C. (B) Biofilm
618 formation of WT *P. fluorescens*. WT GcbC and the catalytically inactive variant (GGAAF) were
619 expressed on plasmids. Experiments were performed in triplicate (± SD), with an indicated P
620 value of either <0.05 (*) or <0.01 (**) with a student's t-test comparing each strain to WT *P.*
621 *fluorescens*. (C) Plasmids containing each of the 21 DGCs and LapD were cotransformed into *E.*
622 *coli* BTH101. After 24 hours of incubation at 30°C, cells were scraped from the plate and β-
623 galactosidase levels were measured to identify LapD interaction partners. Of the 21 DGCs
624 tested, 9 were identified as significantly interacting with LapD by B2H assay compared to the
625 vector only (negative) control. Pfl01_2297, Pfl01_1336, Pfl01_2295, GcbC, Pfl01_4451,
626 Pfl01_2049, Pfl01_4307, Pfl01_2170, and Pfl01_3508 significantly interacted with LapD, but the
627 level of interaction with LapD varied amongst the 9 DGCs. Assays were performed in triplicate
628 with two biological replicates (± SD). Significance was evaluated by a one-way ANOVA analysis
629 followed by a Tukey Multiple Comparison Analysis test, comparing each DGC-LapD interaction
630 to the negative control. Asterisks indicate a P value of either <0.01 (**) or <0.001 (***).

631 **Fig. 5. Identification of potential ligands sensed by Pfl01_2295.** Shown are the results of
632 biofilm assays and B2H assays with the indicated strains and proteins. For each panel, the
633 presence and absence of each organic acid was compared for both biofilm assay and B2H assay.
634 Panel A = +/- succinate; B = +/- acetate. Biofilm assay data are from six biological replicates (±
635 SD). B2H assays were performed in triplicate (± SD). Linear models implemented in R (36) were
636 used to identify organic acid supplemented media whose properties significantly differed from
637 the base medium for both biofilm assay (K10T-1 minimal medium, see Materials and Methods)
638 and B2H assay experiments. P values of <0.05 were considered significant. P<0.01 (**); P<0.001
639 (***). (C) A model of a GcbC, LapD and LapG "basket" signaling complex (25). In this model, the
640 DGC- and PDE-like domains are indicated by the GGDEF and EAL residues typically associated
641 with the active enzymes; we showed previously that these domains of LapD are not active.
642 Instead, the PDE-like domain of LapD binds c-di-GMP (yellow hexagon). The GGDEF domain of
643 GcbC functions as an active DGC in this context. Also indicated are the HAMP signal
644 transduction domain and the S helix of LapD, the CACHE domain of GcbC, the transmembrane
645 (TM) domains, and I-sites (red and orange stars). The LapG pepriplasmic protease is also
646 shown.

647

648 **Supplemental Material.**

649 **Fig. S1. CLUSTAL alignment of the amino acid sequence of the CACHE domain of GcbC and**
650 **rpHK1S-Z16 (PDB ID: 3LIF) of *R. palustris*.** The CACHE domain of GcbC and rpHK1S-Z16 showed
651 31% identity at the amino acid level (E-score = $1e^{-27}$). The red amino acids indicate the
652 conserved residues in the proposed citrate-binding pocket. A subset of these residues are
653 mutated (see Figures 2 and 3 in the main text, and Table S1).

654 **Fig. S2. Effect of a *lapA* mutation on citrate-mediated biofilm formation.** (A) Quantitative
655 analysis of dose-dependent biofilm formation by WT *P. fluorescens* by addition of increasing
656 concentrations of citrate. Citrate concentrations of 0%, 0.4%, and 0.8% were tested. (B)
657 Quantitative analysis of biofilm formation by the WT and *lapA* mutant of *P. fluorescens* in the
658 presence and absence of citrate. (C) Quantification of LapA levels in whole cell lysate in the
659 presence and absence of 0.4% citrate by WT *P. fluorescens* Pf0-1. Representative blots are
660 shown. Data shown is the average of three replicates (± SD). (D) Growth of WT *P. fluorescens* in
661 the presence and absence of citrate for 6 hours at 30°C. (E) Motility by WT *P. fluorescens* in the
662 presence and absence of citrate at 30°C for 30 hours using a soft agar (0.3%) motility assay.
663 Representative images are shown. In all experiments in this figure, assays were performed in
664 triplicate (± SD), and horizontal black bar indicates a P value of <0.05 (*), <0.01 (**), or <0.001
665 (***) by a student's t-test comparing each strain without citrate versus with added citrate, or in
666 panel A, comparing the two different citrate concentrations tested.

667 **Fig. S3. Assessment of DGC activity via congo red binding.** Qualitative analysis of GcbC,
668 Pfl01_2295, and Pfl01_2297 to test for functional c-di-GMP production as described in the main

669 text. These plasmids were transformed into *P. aeruginosa* PA14, and the strains grown on
670 congo red plates supplemented with 0.1% arabinose at 37°C to induce expression of the
671 plasmid-borne DGCs for 24 hours. The binding of red pigment indicates Pel exopolysaccharide
672 production, which serves as an indirect means to assess the amount of c-di-GMP produced by
673 the indicated strain. GcbC and Pfl01_2295 show a higher degree of congo red binding as
674 compared to the empty pMQ72 control and the *pelA* deletion mutant strain. Pfl01_2297
675 showed only a very modest enhancement of congo red binding compared to the empty pMQ72
676 control and *pelA* deletion mutant strain.

677 **Fig. S4. Modeling the CACHE domain of GcbC on rpHK1S-Z16 (PDB ID: 3LIF) and vpHK1S-Z8**
678 **(PDB ID: 3LID)**. Shown is the model of the ligand-binding site of rpHK1S-Z16 (PDB ID: 3LIF) and
679 vpHK1S-Z8 (PDB ID: 3LID), as well as the homology model of the ligand-binding site of the apo-
680 GcbC. On the far right is shown the overall model of the GcbC periplasmic domain based on the
681 structure of rpHK1S-Z16 (PDB ID: 3LIF).

682 **Fig. S5. Identification of ligands sensed by GcbC's CACHE domain.** (A) Shown is a list of organic
683 acids that are color coordinated with the graph in panel B. The chemical structure of acetate,
684 pyruvate, succinate, fumarate, α-ketoglutarate, isocitrate, and citrate are shown. The number
685 of carbon atoms of each compound is listed on the right. (B) Quantitative analysis of biofilm
686 formation by WT *P. fluorescens* and the Δ4DGC mutant strain in the presence of 0.4% acetate,
687 pyruvate, succinate, fumarate, α-ketoglutarate, and isocitrate. The empty vector control and a
688 plasmid carrying GcbC were introduced into the Δ4DGC mutant strain. Biofilm assay data are
689 from six biological replicates (± SD). Linear models implemented in R (36) were used to identify
690 organic acid supplemented media whose properties significantly differed from the base

medium (K10T-1 minimal medium, see Materials and Methods) for both biofilm assay and B2H assay experiments. The reduced biofilm levels for medium supplemented with α-ketoglutarate is due to the poor growth of the strains in the presence of this compound (not shown). P values of <0.05 were considered significant. P<0.05 (*); P<0.001 (***). (C) Biofilm formation by the indicated strains ± isocitrate. The Δ4DGC mutant strain is used with WT GcbC and GcbC-R139E variant introduced on plasmids. For panel C, experiments were performed in triplicate (± SD), and horizontal black bars indicate a P value of <0.05(*) with a student's t-test comparing the presence and absence of isocitrate amongst each strain.

Fig. S6. CLUSTAL alignment of the amino acid sequence of the CACHE domains of GcbC, Pfl01_2295, and Pfl01_2297. The red amino acids indicate the conserved residues of the RXYF motif. The residues highlighted in blue are proposed to make up the putative citrate-binding pocket of the CACHE domain of GcbC. The RXYF motif and residues R139 and R162 of GcbC are conserved in the CACHE domains of Pfl01_2295, Pfl01_2297, and Pfl01_3800.

Fig. S7. Identification of potential ligands sensed by Pfl01_2295. Shown are the results of biofilm assays with the indicated strains. For each panel, the presence and absence of each organic acid was compared for each biofilm assay. Panel A = +/- isocitrate; B = +/- pyruvate; C = +/- fumarate. Biofilm assays are representative of six biological replicates P<0.001 (***).

Table S1. CACHE Domain Mutations.

Table S2. Strains, Plasmids, and Oligonucleotides.

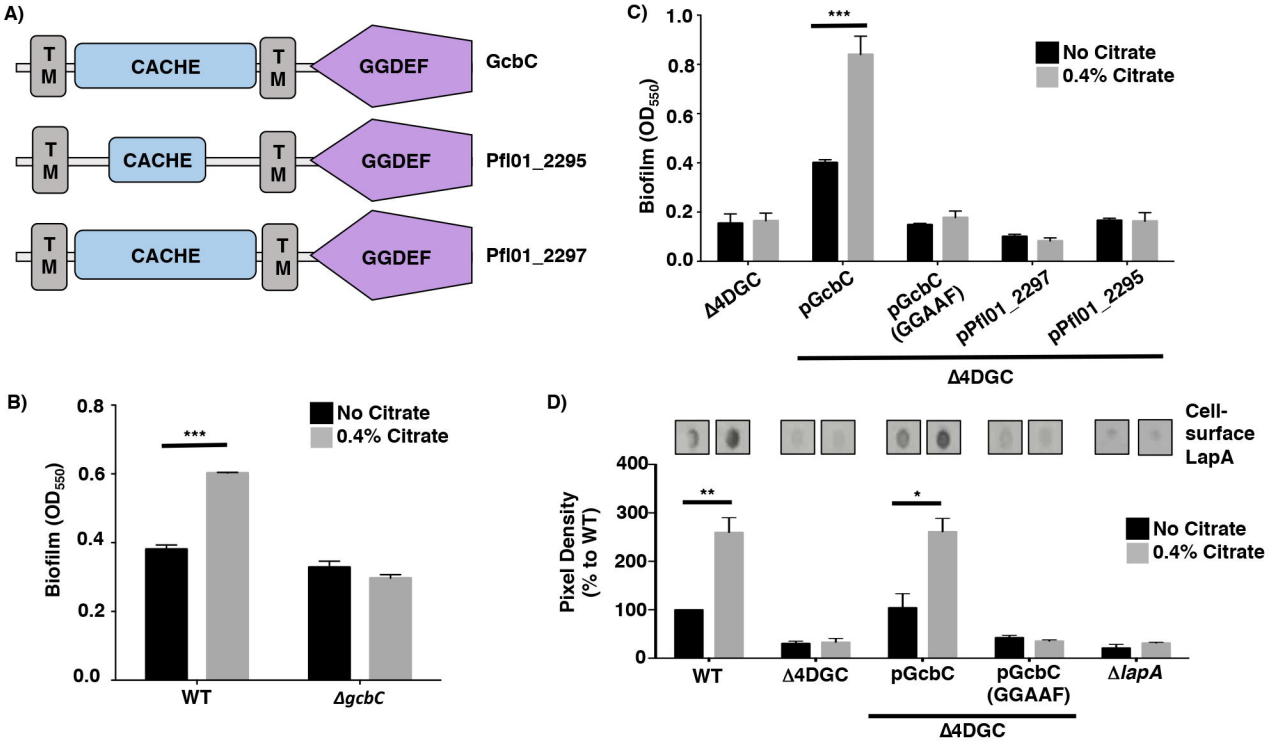
A)
TM
CACHE
TM
GGDEF
GcbC
Pfl01_2295
Pfl01_2297
B)
Biofilm (OD550)
0.8
0.6
0.4
0.2
0.0
***
No Citrate
0.4% Citrate
WT
ΔgcbC
C)
1.0
0.8
0.6
0.4
0.2
0.0
Δ4DGC
pGcbC
pGcbC (GGAAF)
pPfl01_2297
pPfl01_2295
D)
Cell-surface LapA
Pixel Density (% to WT)
400
300
200
100
0
**
*
WT
ΔlapA

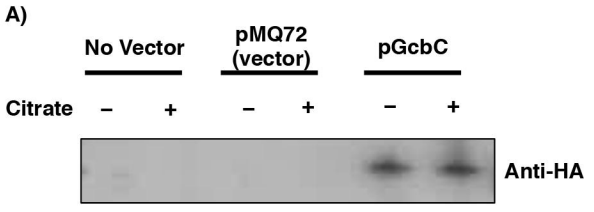
A)
No Vector
pMQ72 (vector)
pGcbC
Citrate
–
+
–
+
–
+
Anti-HA

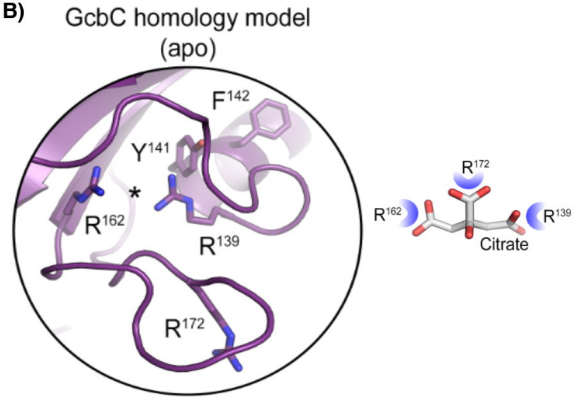
B)
GcbC homology model (apo)
F142
Y141
*
R162
R139
R172
R172
R162
R139
Citrate

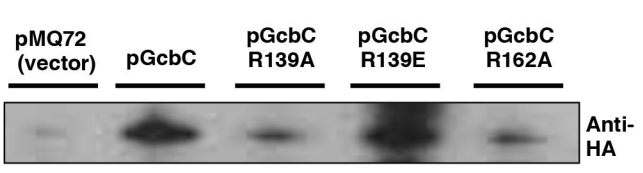
C)
pMQ72 (vector)
pGcbC
pGcbC R139A
pGcbC R139E
pGcbC R162A
Anti-HA

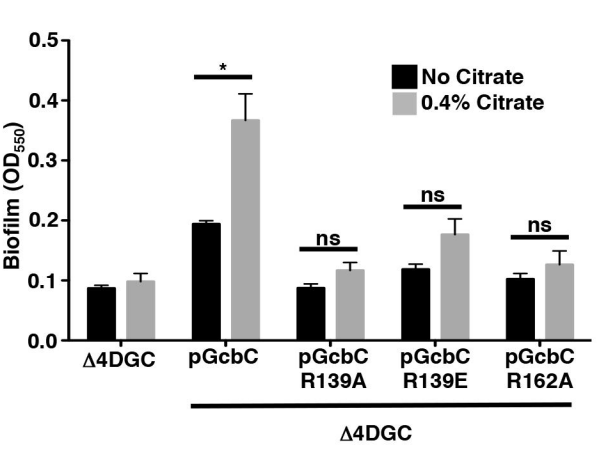
D)
Biofilm (OD_{550})
0.5
0.4
0.3
0.2
0.1
0.0
*
ns
ns
ns
No Citrate
0.4% Citrate
Δ4DGC
pGcbC
pGcbC R139A
pGcbC R139E
pGcbC R162A
Δ4DGC

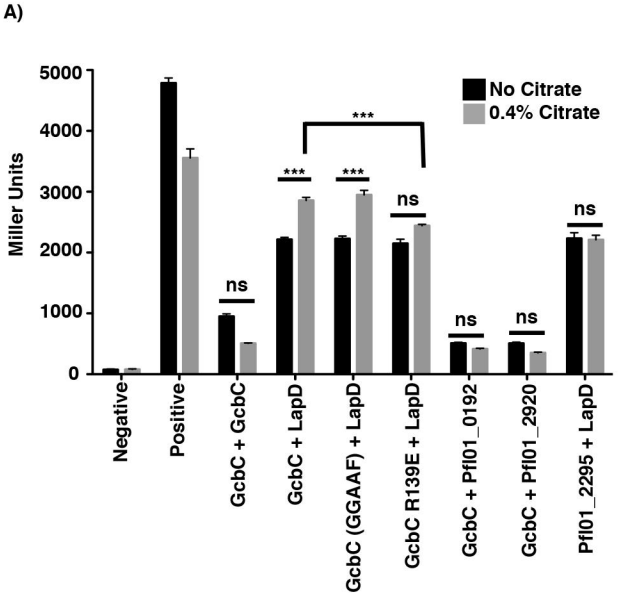
A)
Miller Units
5000
4000
3000
2000
1000
0
No Citrate
0.4% Citrate
***
***
***
ns
ns
ns
ns
ns
Negative
Positive
GcbC + GcbC
GcbC + LapD
GcbC (GGAAF) + LapD
GcbC R139E + LapD
GcbC + Pfl01_0192
GcbC + Pfl01_2920
Pfl01_2295 + LapD

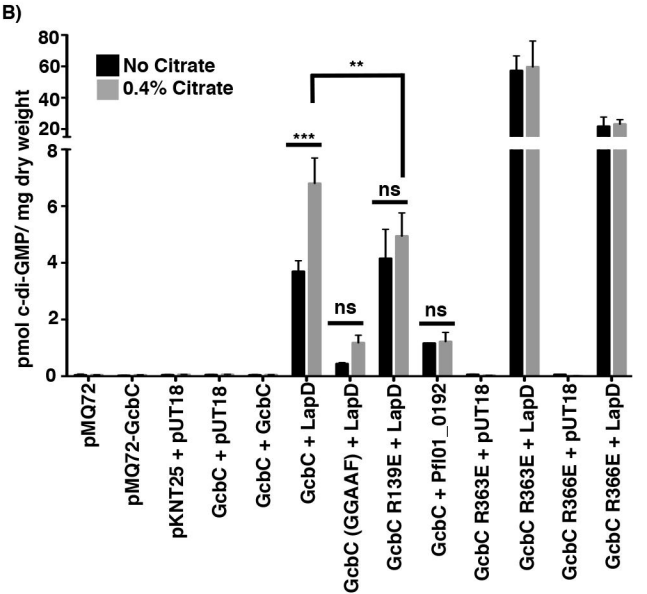
B)
pmol c-di-GMP/ mg dry weight
80
60
40
20
8
6
4
2
0
No Citrate
0.4% Citrate
**
***
ns
ns
ns
pMQ72
pMQ72-GcbC
pKNT25 + pUT18
GcbC + pUT18
GcbC + GcbC
GcbC + LapD
GcbC (GGAAF) + LapD
GcbC R139E + LapD
GcbC + Pfl01_0192
GcbC R363E + pUT18
GcbC R363E + LapD
GcbC R366E + pUT18
GcbC R366E + LapD

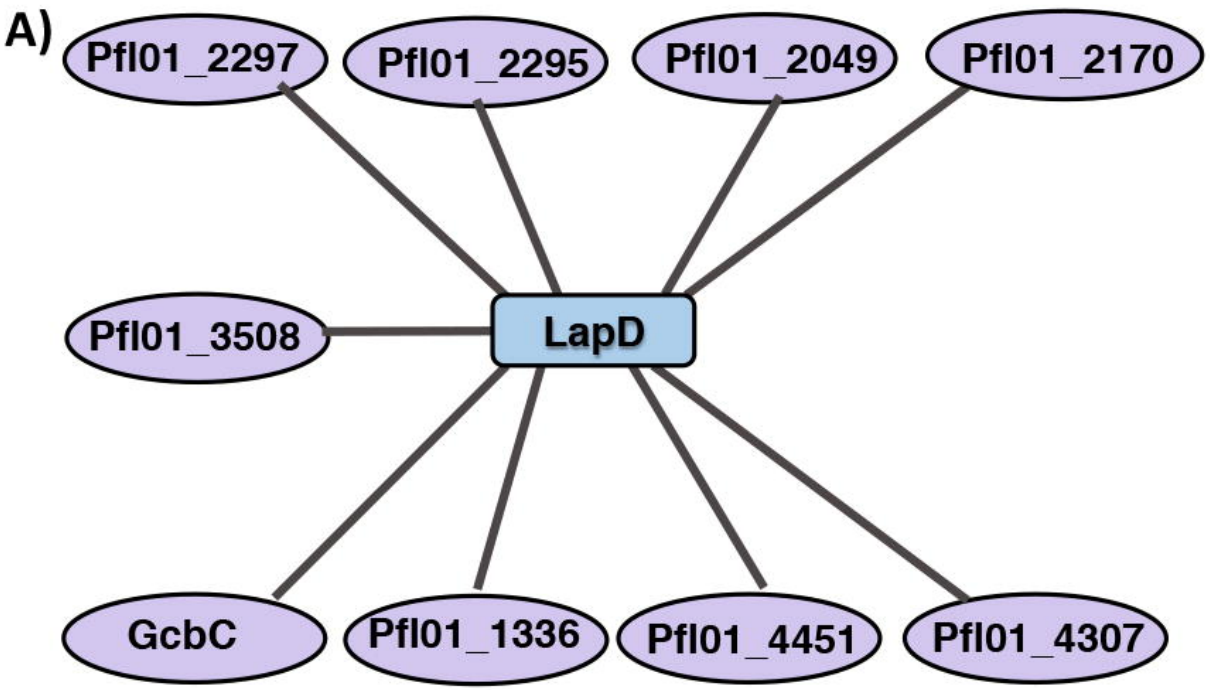
A)
Pfl01_2297
Pfl01_2295
Pfl01_2049
Pfl01_2170
Pfl01_3508
LapD
GcbC
Pfl01_1336
Pfl01_4451
Pfl01_4307

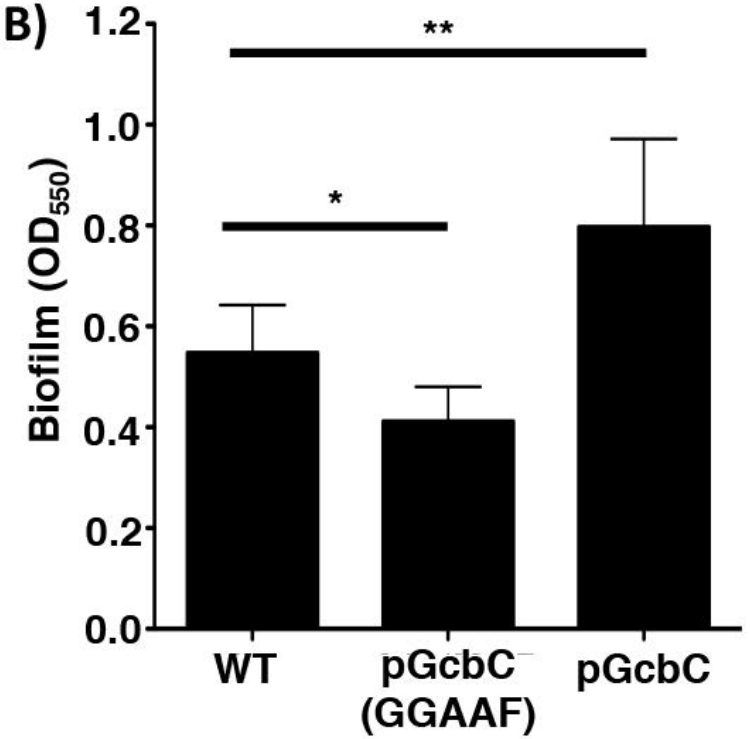
B)
Biofilm (OD_{550})
1.2
1.0
0.8
0.6
0.4
0.2
0.0
**
*
WT
pGcbC (GGAAF)
pGcbC

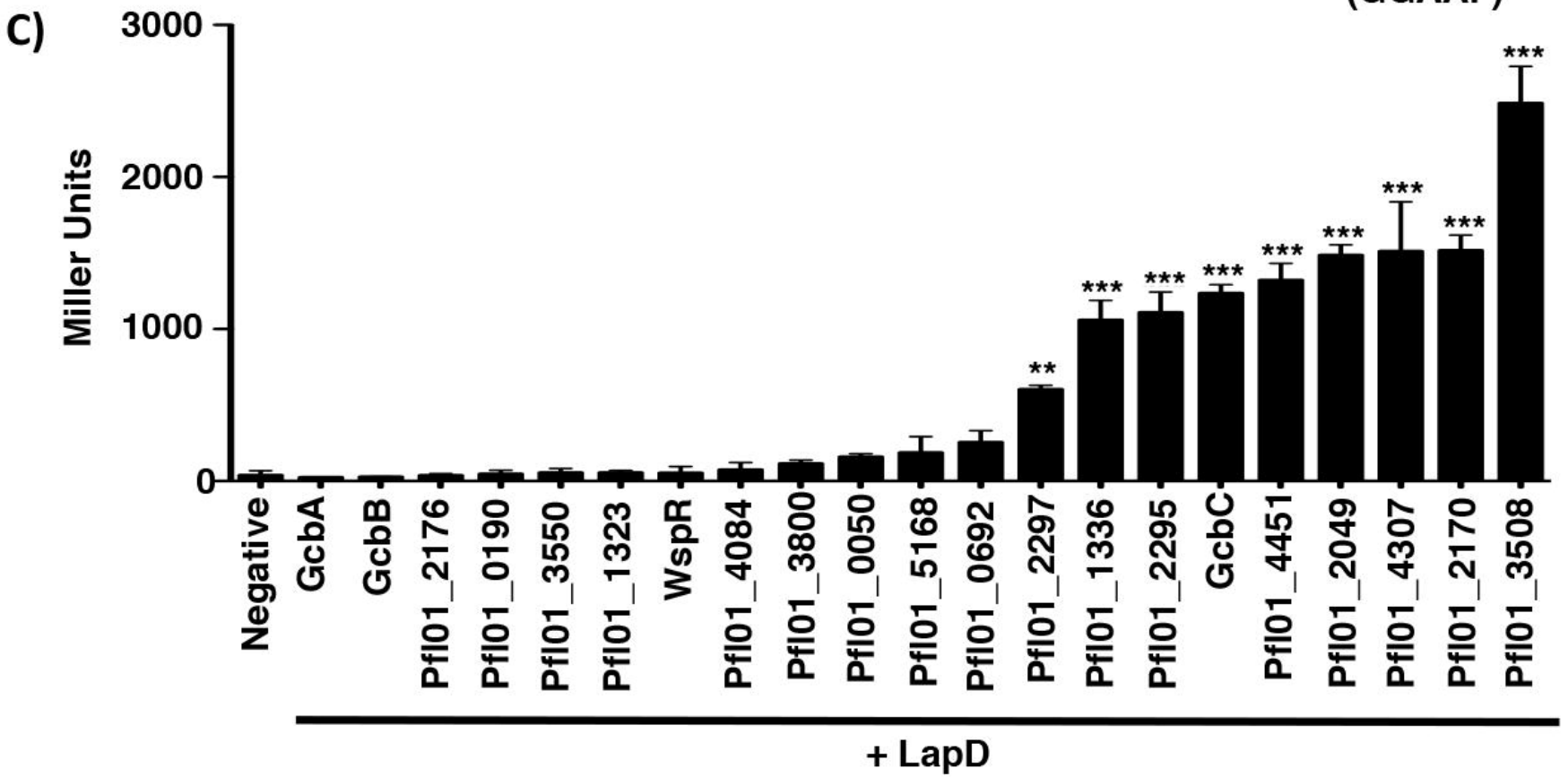
C)
Miller Units
3000
2000
1000
0
Negative
GcbA
GcbB
Pfl01_2176
Pfl01_0190
Pfl01_3550
Pfl01_1323
WspR
Pfl01_4084
Pfl01_3800
Pfl01_0050
Pfl01_5168
Pfl01_0692
Pfl01_2297
Pfl01_1336
Pfl01_2295
GcbC
Pfl01_4451
Pfl01_2049
Pfl01_4307
Pfl01_2170
Pfl01_3508
**
***
+ LapD

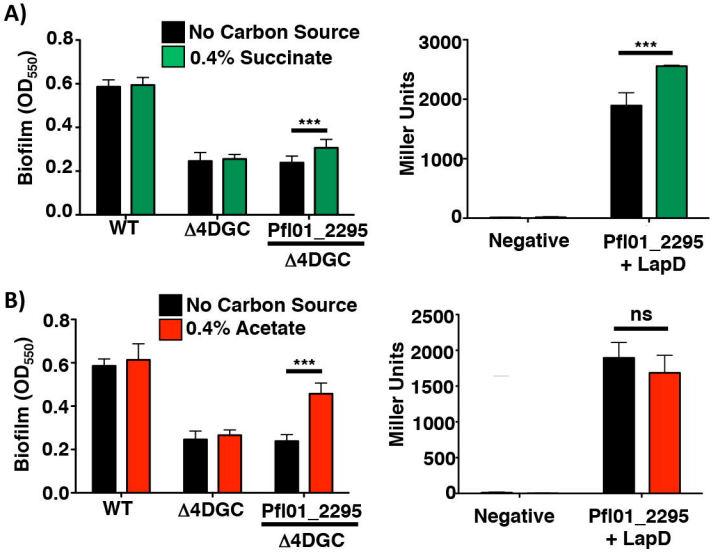
A)
No Carbon Source
0.4% Succinate
Biofilm (OD_{550})
0.8
0.6
0.4
0.2
0.0
***
WT
Δ4DGC
Pfl01_2295
Δ4DGC
Miller Units
3000
2000
1000
0
***
Negative
Pfl01_2295
+ LapD
B)
No Carbon Source
0.4% Acetate
Biofilm (OD_{550})
0.8
0.6
0.4
0.2
0.0
***
WT
Δ4DGC
Pfl01_2295
Δ4DGC
Miller Units
2500
2000
1500
1000
500
0
ns
Negative
Pfl01_2295
+ LapD

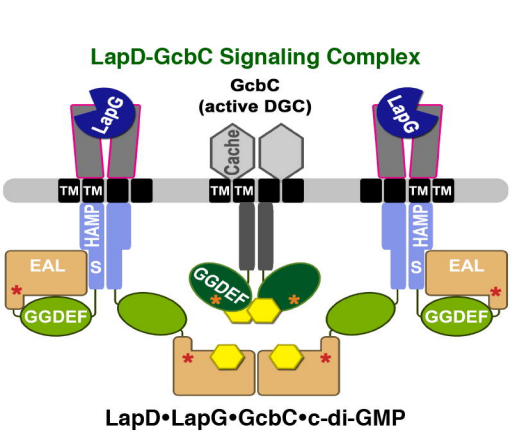
C)
LapD-GcbC Signaling Complex
GcbC
(active DGC)
LapG
LapG
Cache
TM
TM
TM
TM
TM
TM
HAMP
HAMP
S
S
EAL
EAL
GGDEF
GGDEF
GGDEF
LapD•LapG•GcbC•c-di-GMP